First-principles study of the optical transitions of *F* centers in the bulk and on the (0001) surface of α-Al_2O_3

Javier Carrasco, Nuria Lopez, Carmen Sousa, and Francesc Illas*
Departament de Química Física and Centre especial de Recerca en Química Teòrica, Universitat de Barcelona and Parc Científic de Barcelona, C/Martí i Franquès 1, 08028 Barcelona, Spain
(Received 17 February 2005; revised manuscript received 5 May 2005; published 4 August 2005)

The electronic structure and spectroscopic features of the optical spectra of oxygen vacancies in the bulk and on the (0001) surface of α-Al_2O_3 have been studied by first-principles methods. The effect of oxygen vacancies on the crystalline structure has been determined by the appropriate atomic structure optimization carried out using a periodic model and density functional theory (DFT) calculations. Both, neutral (*F* center) and charged (F^+ center) oxygen vacancies have been considered. Optical transitions arising from the excitations of the electron(s) trapped in the F^+ and *F* centers, both on the surface and in the bulk of the material, have been studied using a suitable embedded cluster model approach. The cluster geometry, including the relaxation around the vacancy, has been taken from the periodic calculations. The transition energies and intensities have been obtained by applying the explicitly correlated multiconfigurational second-order perturbation theory method and also time-dependent DFT approaches. The present results are in good agreement with available experimental data for the bulk and provide a guide to interpret forthcoming experiments involving the spectroscopy of oxygen vacancies present in irradiated or defective α-Al_2O_3(0001) surfaces.

DOI: 10.1103/PhysRevB.72.054109 PACS number(s): 61.72.Ji, 78.20.−e, 61.72.Bb, 31.15.Ar

I. INTRODUCTION

Optical spectroscopy has been demonstrated to be a useful tool in the characterization of point defects in ionic materials. This is because the inherent insulator character of these compounds prevents one from applying techniques that make use of charged probes or electric current.[1] Hence, those have been rather restricted to the characterization of insulating oxide thin films or of semiconducting oxides.[2–4] Oxide ultrathin films are often employed as surface models because scanning-tunneling microscopy (STM) and electron spectroscopic techniques can be applied without charging problems. Recently, atomic force microscopy (AFM) has been applied to the study of the alumina surfaces.[5] Nevertheless, one must realize that ultrathin films and regular bulk or surfaces may show very different crystal structures which are not so easy to characterize. This is precisely the case of alumina grown on NiAl(110); it has been very recently proposed that the resulting thin film oxide structure is reminiscent of the κ-Al_2O_3 phase.[6] Even more recently a combined theoretical and experimental study has shown that these ultrathin films deviate from the Al_2O_3 stoichiometry.[7] Therefore, optical spectroscopy still provides a rather unique way to investigate the electronic structure of point defects in the bulk and on the surface of α-Al_2O_3, the most stable crystal phase at normal conditions.

Among the different possible point defects which are present in ionic oxides, oxygen vacancies surely constitute the most important class.[8] Their presence generates colored samples and therefore they have been historically termed *F* centers (from "*Farbe*," color in German) by the spectroscopists. However, removal of oxygen can be either in the chemical form of O or of O^-, leading to *F* and F^+ centers, respectively. Consequently, *F* centers contain two electrons that are trapped in the vacancy due to the strong Madelung potential, while F^+ centers involve a single trapped electron and hence constitute a paramagnetic defect (thus EPR active). In the case of surface oxygen vacancies, more complex structures, for instance involving a single electron trapped and a neighboring H^+ center have been suggested to be better descriptions of the paramagnetic defect on the surface of a simpler oxide MgO.[9]

A deep understanding and characterization of *F* and F^+ centers is fundamental to explain the physics and chemistry of oxides, their role in the chemical properties of catalytic supports, irradiated materials, and optical storage devices, just to mention some potential applications. Hence, the detailed study of these centers is a mandatory step for their practical use and a step towards defect engineering.[8,10] A large amount of experimental data on the spectroscopy of defects in bulk ionic oxides and thin films is available; see, for instance, Ref. 8, and references therein. In the case of bulk oxygen vacancies, the assignment of the corresponding spectroscopic features is rather clear cut. However, in the case of *F* centers located at the surface the situation is more complex since the experimental data usually shows a high dispersion and is strongly affected by the sample history. Consequently, the assignment of the corresponding optical bands is in most of the cases far from being straightforward. In particular, the experimental optical spectroscopic features of oxygen vacancies of bulk irradiated α-Al_2O_3 samples have been deeply analyzed.[11–15] For the *F* center, the optical spectrum is dominated by a single absorption band centered at 6.05 eV and, which within the C_2 point symmetry group, corresponds to a $1A \rightarrow 2A$ transition. The F^+ center shows two different band centers at 4.8 and 5.4 eV, respectively, and a third one, at 5.95 eV revealed by the time-resolved spectra of the optical excitation; the latter partially overlaps the *F* center absorption band. These have been assigned to

$1A \rightarrow 1B$, $1A \rightarrow 2A$, and $1A \rightarrow 2B$, respectively. Emission from F^+ takes place at 3.8 eV (Ref. 15) while decay of excited F states is a much more complex phenomenon that might also involve the $F \rightarrow F^+$ deactivation channel. No experimental information is available concerning the spectroscopic features of surface related oxygen vacancies in α-Al_2O_3. Previous theoretical studies in the literature report either point ion[16] or semiempirical[17] calculations on cluster models simulating oxygen vacancies in bulk corundum. In the present work, we extend these pioneering studies by applying the atomistic first-principles methods to both bulk and surface oxygen vacancies and at the same time evaluate the predictive capability of these theoretical methods.

The theoretical interpretation of the optical spectra arising from excitations of electrons trapped at the cavities left by oxygen vacancies has been possible only very recently.[18–20] Nowadays, theoretical modeling has reached enough accuracy to become crucial in the systematization of the experimental observations and, in some cases, provides the proper assignment of the spectroscopic fingerprints of these point defects. For example, the spectroscopic features of O vacancies in MgO bulk and at the MgO(001) surface have been investigated at length. In this simple material, the very small geometric relaxation around the vacancy, as predicted either by cluster model[21] or periodic calculations,[22] and the strongly localized nature of the ground and excited states related to the trapped electrons left upon oxygen removal[21,23] was profited to define a properly embedded cluster. The main advantage of cluster models to periodic supercell approaches is that on the former sophisticated, explicitly correlated, *ab initio* wave-function-based methods can be applied simultaneously to the ground and excited states These techniques allow one to compute the energy transitions from the ground to the low-lying excited states and the corresponding oscillator strengths, thus providing information for the proper assignment of the spectroscopic features of interest. More recently, density functional techniques in the time-dependent formulation (TD-DFT) have also been applied to study excited state related problems in oxide surfaces.[24–26] However, these schemes have been claimed to show a somehow erratic behavior in the description of the spectroscopic features of oxygen vacancies in MgO.[25] More recent investigations have shown their utility connected to alkali photoemission in silicate samples if a proper investigation of boundary effects is done.[26]

The aim of the present study is to extend previous work on the structure and stability of surface and bulk α-Al_2O_3 neutral F centers[27] by including the structural study of the bulk and surface charged F^+ point defects and the spectroscopic features of bulk and surface F and F^+ centers. To this end, we combine different models—periodic models and embedded clusters—representing bulk and surface oxygen vacancies of α-Al_2O_3 and state of the art theoretical methods—TD-DFT and explicitly correlated wave functions—to predict and assign the optical absorptions corresponding to the defective F and F^+ centers in both bulk and at the (0001) surface of corundum.

II. MATERIAL MODELS AND COMPUTATIONAL METHODS

A. Periodic calculations

The structure of F and F^+ centers in the bulk and on the (0001) surface of α-Al_2O_3 has been determined by means of periodic density functional theory calculations applied to sufficiently large supercells so that the interaction between point defects can be safely neglected. The optimum unit cell parameters consistent with the energy calculation method described below have been used for the periodic calculations. The positions of the atoms surrounding the missing oxygen (F and F^+) both in the bulk and at the surface supercell has been reoptimized as done previously.[27] Except for the F^+ center, the computational details and structural results concerning the periodic calculations are the same employed recently for the study of bulk and surface F centers of corundum.[27] For the surface, the Al-terminated (0001) plane has been chosen since it is well established that this is the equilibrium termination for the clean α-Al_2O_3(0001) surface.[28] Nevertheless, it is worth pointing out that this surface is rather difficult to obtain experimentally due to its rapid hydroxylation.[29,30] The surface O-vacancy models have been obtained by removing a single O atom (or O^- anion) from the relaxed, hydroxyl-free structure. The energies have been determined using the Perdew-Wang (PW91) implementation[31] of the exchange-correlation functional, this functional belongs to the family of methods developed under the so-called generalized gradient approximation (GGA). Inner electrons have been represented by the Blöchl's projected augmented wave (PAW) method.[32] This is essentially a frozen-core all-electron-like approach that combines the accuracy of all electron methods with the computational simplicity of the pseudopotential approach. This is particularly true in the implementation of Kresse and Joubert.[33] The use of this approach permits one to obtain accurate results with an energy cutoff of 415.0 eV.

For the bulk structure, the obtained cell parameters for α-Al_2O_3 are essentially the same previously determined values and are in very good agreement with experiment.[27,34] Defective bulk structures have been studied using $3\times3\times1$ and $2\times2\times1$ unit cells for F and F^+ centers, respectively. In the latter case, calculations have to be carried out using the spin polarized formalism which computationally is exceedingly demanding for the $3\times3\times1$ supercell and consequently a smaller unit cell needs to be used. However, previous studies have shown that for unit cells as those indicated above there is almost no interaction between the repeated defects.[34] In fact, since the unit cell vectors are the same as for the bulk, without any rotation, the defects are separated at least by 13.1 Å in the z direction and the minimum distance along the xy plane is either 9.6 Å ($2\times2\times1$) or 14.4 Å ($3\times3\times1$). A Monkhorst-Pack grid with a $2\times2\times1$ special k point scheme has been used for the integration in the reciprocal space. For the charged F^+ defect, the extra charge has been compensated through an appropriate uniform background so that the final cell is neutral.

In the case of surface defects, the electric dipole between repeated images has been eliminated using the standard

approach.[35] To describe oxygen vacancies at the surface, a repeated slab consisting of six Al-O-Al units (18 atomic layers) separated with a 12 Å of vacuum width has been used. For both bulk and surface defects, the effect of coupling between repeated cells has been investigated by monitoring the defect formation energy with respect to the size of the supercell. The obtained results evidence that the supercells described above, which correspond to a 1% defect concentration, are sufficiently large. All periodic calculations have been carried out using a parallel version of the VASP code[36] implemented on an IBM SP4 computer and in Linux clusters.

B. Embedded cluster models

The spectroscopic features related to bulk and surface F and F^+ point defects of α-Al_2O_3 have been studied using properly embedded cluster models. These models are defined such that a local part of the material is described by quantum-mechanical methods while the effect of the rest of the crystal in the local region is taken into account in a more approximate way.[37,38] There is compelling evidence that these models are adequate to describe many local properties of ionic oxides[8] including excited states[39] and magnetic properties.[40–42] This is because, on the one hand, cluster models allow one to use very accurate, explicitly correlated, wave function based methods and, on the other hand, compared to periodic models, provide a better representation of the low concentration of point defects in the real samples, i.e., no coupling between defects is present. Modeling ionic solids by cluster models usually proceeds in well established three-shell embedding scheme. Thus, the innermost shell contains the atoms directly involved in the property of interest and are described fully quantum mechanically. The second shell contains a set of atoms which are aimed to account for the electrostatic and Pauli repulsion with the atoms in the first shell. The centers on the second shell are modeled by effective core potentials (ECPs), those potentials carry no electrons but have the corresponding formal charge of the corresponding cation or anion. Finally, the outermost shell contains an array of point charges accounting for the long-range Madelung potential. The second layer avoids the spurious polarization that would create the presence of point charges in the neighborhood of strongly polarizable oxygen anions. The set of centers represented as point charges, having fully ionic values (+3 and −2), has been generated from the clean crystal bulk structure in such a way that they are centered in an O atom. The Madelung potential in the region where this central O atom is placed is evaluated through the standard Ewald procedure.[43] Next, arrays of point charges contained in concentric spheres of increasing radii are selected in such a way that the Madelung potential is well reproduced and the total charge of the system thus constructed is zero.[44] Therefore the final system is neutral for the F models while it has a single positive charge for F^+ models. A similar procedure has been performed to build cluster models containing the surface vacancies which takes into account the surface relaxation predicted from the corresponding slab calculation.[44] In all cases the final structure around the vacancy is introduced using the output of the periodic calculations. The final cluster model contains a vacancy (vac) in the site where the central O atom was located. The first shell contains the vacancy plus the next neighboring Al and O atoms giving rise to a $(vac)Al_4O_{16}$ and to $(vac)Al_3O_{11}$ cluster models for bulk and surface, respectively. The 26 (16) cations for bulk (surface) surrounding the border anions in the cluster are represented by total ion potentials (this is achieved by using atomic pseudopotentials); see Fig. 1. The arrays of point charges include 9096 and 4676 ionic sites for the bulk and surface, respectively.

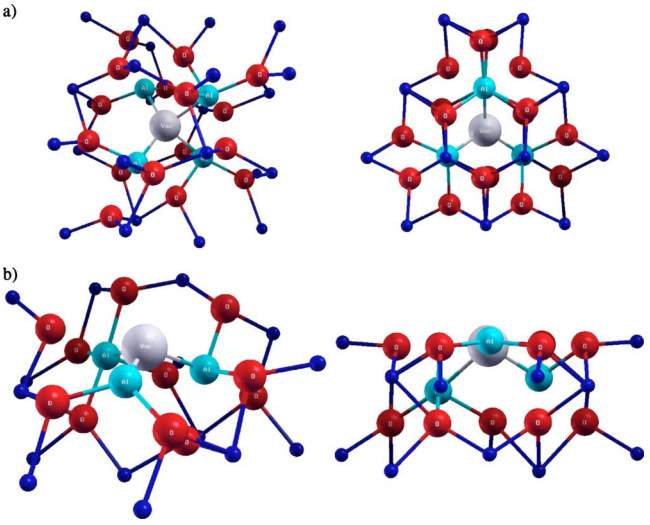

FIG. 1. (Color online.) Cluster models employed in the TD-DFT and CASPT2 calculations for the defective F and F^+ centers of α-Al_2O_3 (a) bulk, (b) (0001) surface. Left: tridimensional view and right: lateral view. In red: oxygen atoms, blue: Al cations, dark blue: Al pseudopotentials, grey: vacancy. The array of point charges is not displayed.

C. Methods employed for the study of excited states on cluster models

The clusters described in the previous section, including the relaxation predicted by the periodic supercell calculations, have been used to carry out time-dependent density functional theory (TD-DFT) calculations aimed at investigating the low-lying excited states. The TD-DFT calculations have been performed with the hybrid B3LYP (Ref. 45) exchange-correlation functional to provide vertical transition energies and oscillator strengths to the low-lying excited states. For the TD-DFT calculations, the density was expanded in a Gaussian basis set. In particular, the 6-31G^* basis has been chosen for Al atoms while for O a basis set optimized for O^- has been used $(4s,2p,1d)$.[46] Although not mandatory, a ghost basis placed at the vacancy has been used because it has been shown to provide a good way to characterize and analyze the transitions and to speed up the convergence.[18–20,25] Therefore, the same O basis has been placed at the positions of the missing oxygen atoms. The Al ECP reported by Hay and Wadt[47] has been used to represent the Al^{3+} cations around the edge O atoms in the cluster. From

all the excitation energies issued from the TD-DFT calculations, only those involving impurity states close to the conduction band show oscillator strengths large enough to be considered as responsible for the experimentally observed bands. The stability of the TD-DFT results with respect to the basis set quality has been checked by repeating all calculations using the Ahlrichs' valence triple-ζ (Ref. 48) augmented with the polarization functions provided in the Ahlrichs' double-ζ plus polarization basis set,[48,49] this basis set will be denoted as VTZ-P. As it will be shown in the forthcoming discussion, the excitation energies and oscillator strengths calculated with the two basis sets are almost indistinguishable. Cluster model TD-DFT calculations have been carried out by means of the GAUSSIAN98 package.[50]

In order to check the predictions of TD-DFT, the ground and low-lying excited states have also been computed using a well defined, wave function based, method which has a longer tradition in the study of excited states. In the present work, the complete active space second-order perturbation theory (CASPT2) (Refs. 51 and 52) method has been applied to the cluster models employed in the TD-DFT calculations. In this approach an important part of the nondynamical electron correlation effects is treated variationally by computing the complete active space self-consistent field (CASSCF) wave function, and the remainder, mainly dynamical electron correlation, is estimated by second-order perturbation theory with the CASSCF as zeroth-order wave function. This strategy combines the accuracy of a multireference configuration interaction treatment and the low computational cost of a perturbational approach. Indeed, CASPT2 has been successfully applied to study excited states in solid state compounds.[53–58]

The active space used to construct the reference CASSCF wave functions includes the four vacancy orbitals involved in the lowest transitions, namely, one *s*-type and the three components of the *p*-like orbital, and two or one electron for the F and F^+ centers, respectively.[20] The CASSCF wave functions have been optimized for an average of the lowest four low-lying states, i.e., in a state-average CASSCF calculation. In the subsequent multistate CASPT2 calculation all O and Al valence electrons are correlated. In order to systematically investigate the performance of this method, several basis sets have been used. First, for comparison purposes, the same basis set used in the TD-DFT calculations has been employed. However, as the degree of dynamical electron correlation included in the wave function based calculations appears to be very sensitive to the quality of the basis set, it increases when increasing the basis set size, CASPT2 calculations have been carried out using basis sets of increasing size. In particular, a rather large series of ANO type basis sets has been employed for Al and O although for simplicity results will be reported for two basis sets hereafter referred to as small (S) and large (L), respectively. Basis S consists of a $(3s2p)$ basis for Al and $(3s2p1d)$ for O whereas basis L is $(4s3p)$ for Al and $(4s3p1d)$ for O. Both sets include a segmented $(3s2p1d)$ basis for vacancy as employed in previous works.[18–20] Moreover, in the CASPT2 calculations two different embedding schemes have been used. The first one corresponds strictly to the one described above and used in the TD-DFT calculations. In the second one, not only the Al cations were considered, but also the O^{2-} ions were replaced by *ab initio* model potentials in such a way that the second shell of the embedding scheme extends 10 Å around the vacancy.[59] This second embedding scheme provides a better description of the system and, in addition of preventing the electron density to flow to the point charges, incorporates the finite size effect of all ions on the second shell.

Finally, it is worth pointing out that in the CASSCF/CASPT2 approach, the oscillator strengths are computed making use of the transition dipole moments derived from the CASSCF wave functions and the CASPT2 excitation energies. The CASSCF/CASPT2 calculations have been performed using the MOLCAS 5.4 package.[60]

III. RESULTS AND DISCUSSION

A. Geometric and electronic structure upon vacancy creation

The energy needed to create F centers on corundum is rather large as found for other ionic oxides such MgO.[8,34] Periodic DFT calculations predict F center formation energies of $\sim$10 eV for the bulk and only 10% less for the α-$Al_2O_3(0001)$ surface; both calculated with respect to $O(^3P)$ as estimated by an appropriate spin-polarized calculation in a slightly distorted cubic box.[27,34] Since corundum is essentially an ionic oxide,[61] and the creation of a surface does not represent changes in the ionic character of this material,[62,63] the electron(s) left upon removal of atomic oxygen or of O^- are sufficiently localized in the vacancy cavity[27] because of the large value of the Madelung potential around this site. Nevertheless, the vacancy formation induces a considerable structural relaxation. Absolute and relative displacements with respect to the ideal structure are shown in Table I for the F and F^+ centers in both the bulk and at the surface. For the F centers, results are identical to those published in an earlier work[27] and are only introduced here for comparative purposes. For both types of point defects either in bulk or surface, first and second nearest neighbors have been allowed to relax. A significantly different behavior is found for F and F^+ centers. Hence, for neutral F centers in bulk and surface an inward relaxation of the first shell of atoms around the vacancy appears whereas around F^+ centers the relaxation of these atoms is outwards. This behavior can be explained as arising from the electrostatic interaction reduction when passing from a neutral F center (two electrons trapped) to a charged F^+ center (one electron trapped). The degree of relaxation is larger on the surface as expected from the reduced coordination. The local structure around the vacancies predicted by the supercell periodic calculations has been used to construct the cluster models employed for the spectroscopic calculations. These clusters are shown in Fig. 1.

The electronic structure of bulk corundum predicted by the PW91 exchange-correlation functional has been discussed at length in a previous work.[27] Here, let us just point out that the calculated band gap is too small as found for other ionic oxides.[64] In fact, the PW91 band gap is of 5.9 eV, much smaller than the experimental value of 8.7 eV.[65,66] The introduction of a part of non-local exchange as done in the hybrid B3LYP functional results in a significant improvement

TABLE I. Absolute (Δr) and relative (%) atomic displacements of the ions at distances less than 3 Å from the F or F^+ oxygen vacancy in bulk and (0001) surface of α-Al_2O_3.

	F				F^+			
	Bulk		Surface		Bulk		Surface	
	Δr/Å	%	Δr/Å	%	Δr/Å	%	Δr/Å	%
Al	−0.096	−5.40	−0.200	−13.3	0.117	5.9	−0.058	−3.8
Al	−0.096	−5.40	0.015	0.8	0.117	5.9	0.142	7.7
Al	0.018	0.87	0.125	6.2	0.105	5.0	0.207	10.2
Al	0.018	0.87			0.105	5.0		
O	−0.016	−0.63	−0.037	−1.4	−0.056	−2.2	−0.055	−2.1
O	−0.016	−0.63	−0.065	−2.5	−0.056	−2.2	−0.078	−3.0
O	−0.003	−0.11	−0.053	−2.1	−0.027	−1.0	−0.075	−2.9
O	−0.003	−0.11	−0.017	−0.6	−0.026	−1.0	−0.097	−3.6
O	−0.012	−0.46	−0.007	−0.3	−0.041	−1.5	−0.021	−0.8
O	−0.012	−0.46	−0.050	−1.9	−0.040	−1.5	−0.051	−1.9
O	−0.001	−0.06	0.000	0.0	−0.026	−0.9	−0.055	−2.0
O	−0.001	−0.06	−0.049	−1.7	−0.025	−0.9	0.005	0.1
O	−0.010	−0.33	−0.080	−2.8	−0.009	−0.3	−0.042	−1.5
O	−0.010	−0.33			−0.009	−0.3		
O	0.000	0.00			−0.003	−0.1		
O	0.000	0.00			−0.004	−0.1		

of the calculated band gap, 8.5 eV as predicted from B3LYP periodic calculations[67] and 9.9 eV as estimated here from TD-DFT within the B3LYP method but using the cluster model approach. The inclusion of a single vacancy in the supercell results in a narrow impurity band in the gap which evidences again the local nature of the electronic states corresponding to the trapped electron(s).

B. Spectroscopic features of bulk vacancy centers

Next, we focus on the low lying excitations allowed by the dipole selection rule which are related to the F or F^+ center electrons. Calculated excitation energies are compared to the experimental values obtained in spectroscopic measurements. Results for the bulk F and F^+ centers, as predicted by TD-DFT and CASPT2 cluster model calculations, are reported in Table II. For the F center, the three low lying excitations always appear in a narrow range of energy. This is in agreement with the appearance of a single band in the experimental spectrum.[14] On the contrary, for the F^+ center, the three low-lying excitations are rather well separated, also in agreement with experimental findings. Nevertheless, even if the separation between the different calculated excitations closely follows the separation between the experimental peaks, the numerical coincidence between the experimental and calculated values depends on the method used; the TD-DFT results being in general closer to experiment. An analysis of the wave functions corresponding to the initial and final states reveals that the electronic transitions reported in Table II can be understood as one-electron excitations from

TABLE II. Lowest electronic transition energies (T_e, in eV) and transition probabilities (f) for the most relevant transitions arising from O-deficient sites in bulk α-Al_2O_3 as predicted by TD-DFT and CASPT2 methods.

		Experiment (Refs. 11–15)	TD-DFT				CASPT2					
			6-31G^*		VTZ-P		6-31G^*		Basis S		Basis L	
System	Transition	T_e	T_e	f	T_e	f	T_e	f	T_e	f	T_e	F
Bulk F	$1A \rightarrow 2A$	6.05	6.19	0.41	6.16	0.39	6.59	0.54	6.84	0.61	6.86	0.59
	$1A \rightarrow 1B$		6.20	0.42	6.23	0.40	6.57	0.55	6.97	0.62	7.01	0.60
	$1A \rightarrow 2B$		6.45	0.17	6.48	0.20	7.03	0.44	7.57	0.49	7.53	0.49
Bulk F^+	$1A \rightarrow 1B$	4.8	4.86	0.24	4.84	0.24	5.31	0.32	5.31	0.36	5.43	0.34
	$1A \rightarrow 2A$	5.4	5.30	0.22	5.31	0.22	5.87	0.32	6.01	0.35	6.10	0.33
	$1A \rightarrow 2B$	5.95	5.94	0.13	5.93	0.13	6.67	0.28	6.96	0.29	6.99	0.29

an orbital strongly localized in the vacancy with an almost spherical shape (*s*-like) to orbitals also localized in the cavity but exhibiting a nodal plane (*p*-like) and hence closely related to the *p* atomic symmetry. This is consistent with the existence of three low lying states either for the *F* or F^+ centers and with the $s \rightarrow p$ notation used by some authors.[14] For the F^+ center this is also consistent with the fact that these excitations are sensitive to the light polarization.[11] Indeed, the lowest $1A \rightarrow 2A$ corresponds to an excitation to a p_z-like orbital since it shows up only with light polarized in the direction perpendicular to the *c* axis. On the contrary, the $1A \rightarrow 1B$ and $1A \rightarrow 2B$ appear when the exciting light is polarized in direction parallel to c and can be assigned to excitations to the p_x- and p_y-like orbital.

Nevertheless, the more open structure of the corundum compared to rocksalt oxides has two effects which have to be stressed. First, compared to *F* centers on MgO, the lower point group symmetry leads to three nonequivalent *p*-like states. Second, in corundum, the degree of localization of the trapped electrons in either ground or low lying excited states is clearly lower. A final general comment concerns the relative intensities of the *F* and F^+ excitations as predicted from the calculated oscillator strength. Both, TD-DFT and CASPT2 methods predict relative intensities for the *F* center excitations which are nearly twice the value corresponding to the F^+ center excitation. This is in agreement with the behavior observed for the alkaline earth oxides.[12]

Next, we discuss in more detail the performance of the different theoretical methods. The qualitative picture provided by TD-DFT and CASPT2 calculations is essentially the same, although the latter exhibit a larger error with respect to experiment. The first striking feature of TD-DFT results is its insensitivity with respect to the basis set quality. In fact, results obtained using the standard 6-31G^* basis or using the more extended VTZ-P basis is almost indistinguishable. A more outstanding achievement of the TD-DFT results is the almost perfect coincidence with experimental bands for both *F* and F^+ centers, including the three different bands relatively close in energy from 4.8 to 6 eV. The F^+ lowest transition occurs at energies 1.3–1.5 eV lower than that of the *F* center. Notice that this in contrast to bulk MgO where the measurements indicate that *F* and F^+ excitations are almost coincident. Since, the B3LYP TD-DFT approach has only been tested in a few cases we find it convenient to further check the results with a robust and well established method. Calculations carried out using the CASPT2 method evidence a somewhat larger dependence with respect to the basis set quality, as expected,[20] and also a larger deviation from experimental values. This is in the line of previous studies concerning *F* and F^+ centers excitations in MgO.[18–20] The difference between CASPT2 and experimental values is in the 0.5–1.0 eV energy range, again similar to that found for MgO and shown to be due to the use of a relatively small basis set.[20] However, in the case of α-Al_2O_3 the situation appears to be more complex because of the interplay between basis set quality and embedding. In fact, in the case of MgO, the cubic symmetry of the system leads to a rather close packed environment around the oxygen vacancy and extending the basis set does not place electron density outside the vacancy region. However, in the case of corundum the crystal structure is more open and extending the basis set leads to electron density in the region near the second shell of oxygen atoms which are now described as point charges. Treating these second shell of oxygen atoms as well as the corresponding aluminum ones as *ab initio* model potentials has a noticeable 0.25 eV decrease on the excitation energies computed with large basis sets. However, the effect is the same for all computed excitations and hence has not implications for the discussion and assignment of the low-lying electronic transitions. Nevertheless, improving basis set quality and embedding scheme in the CASPT2 calculations results in values which systematically approach the experimental value. However, the high computational cost of such wave function based methods precludes a routine use, especially for such large cluster models.

Finally, we comment on the role of structural relaxation in the calculated spectroscopic features. For *F* centers in MgO the relaxation in the vacancy neighborhood is small and hence it has been found to have only a minor effect on the calculated excitation energies.[18,19] However, in corundum the extent of relaxation is significantly larger and therefore the effect of structural relaxation on the excitation energies will also be larger. In fact, additional TD-DFT calculations carried out for the F^+ center at both the *F* and the F^+ optimized geometries show that the transition energies can be lowered by as much as 0.8 eV when the change in geometry is taken into account. Notice, however, that the relaxation of first and second atomic shells around *F* and F^+ is in the opposite direction. Therefore, as expected, the excitation energy increases when the structure is compressed.

C. Spectroscopic features of surface vacancy centers

As pointed out in the introduction, the alumina surface in the corundum phase is most likely hydroxylated.[29] Moreover, no UV or similar spectroscopic studies have been reported for the clean or hydroxylated surface that may be related to surface *F* centers. Since the main interests of this work is to identify the role of the vacancy coordination and relaxation in the excitation energies only the simplest clean surface has been considered. First of all, the reduced coordination on the surface splits the nearly degenerate excited states of the bulk *F* center and, consequently, the excitation energies also split; one to lower transition energies centered at ~4.6 eV and two to values larger than 6 eV; comparable to those discussed above for bulk *F* centers (Table III). The same trend appears for the surface F^+ center although here the excited states are already separated in the bulk. The strong relaxation which leads to three nonequivalent Al cations surrounding the vacancy, and which has been discussed at length in a previous work,[27] completely removes the point symmetry. This is the origin of the energy level splitting. Nevertheless, the more complex structure of corundum precludes a more detailed analysis. A similar behavior has been found in MgO (Ref. 68) which is well reproduced by theoretical calculations.[19] This effect has also been recently suggested for similar point defects in alkali halides.[69] The combined effect of coordination loss and enhanced relaxation leads to rather large differences between surface and bulk *F* center excitations;

TABLE III. Lowest electronic transition energies (T_e, in eV) and transition probabilities (f) for the most relevant transitions arising from O-deficient sites in α-Al_2O_3(0001) as predicted by TD-DFT and CASPT2 methods.

	TD-DFT				CASPT2					
	6-31G^*		VTZ-P		6-31G^*		Basis S		Basis L	
System	T_e	f	T_e	f	T_e	f	T_e	f	T_e	f
Surface F	4.62	0.23	4.62	0.24	4.56	0.37	5.21	0.36	5.03	0.34
	6.24	0.25	6.36	0.23	6.60	0.20	7.34	0.50	7.07	0.47
	6.63	0.20	6.68	0.10	6.65	0.30	7.54	0.61	7.31	0.51
Surface F^+	4.50	0.14	4.49	0.14	4.97	0.24	5.02	0.26	5.21	0.26
					6.68	0.27	7.10	0.28	6.99	0.29
					7.30	0.31	7.72	0.34	7.56	0.34

$\sim$1.7 eV for the F center and still important for the paramagnetic defect 0.4–0.2 eV for TD-DFT and CASPT2, respectively. As for the bulk point defects, CASPT2 predicts excitation energies which are larger than those arising from TD-DFT but again the important point is that both methods consistently predict the same trend. Notice than both TD-DFT and CASPT2 methods predict that electronic transitions for the surface F centers have intensities which are half those of the bulk. For the surface F^+ center only a band has been calculated with TD-DFT corresponding to a transition energy of 4.5 eV and, again, with a much smaller intensity than the corresponding to the bulk. Interestingly, the difference between the band positions for surface F and F^+ centers is much smaller than for the bulk F and F^+; 0.3 or 0.2 eV for TD-DFT and CASPT2, respectively. As commented for the bulk defect, the relaxation also affects the position of the band and, as for the bulk; the transition takes place at lower energies with the F^+ geometry by 0.3 eV.

IV. CONCLUSIONS

The optical properties related to electron(s) trapped at O vacancies in bulk and (0001) surfaces of α-Al_2O_3 have been studied by means of state-of-the-art *ab initio* quantum chemical methods applied to suitably embedded cluster models. In order to introduce the main structural effects in the cluster models, periodic calculations using sufficiently large supercells have been carried out and the resulting geometry used to build the cluster models. The electronic excitations derived from the trapped electrons are found to have a quite strong intensity. Moreover, for the bulk F and F^+ centers, a good agreement with the observed spectroscopic features is found. This agreement is especially excellent for the TD-DFT calculations. Both TD-DFT and CASPT2 methods report very similar results thus providing increasing confidence in the new TD-DFT–based methods. The present TD-DFT results obtained using well-balanced basis sets, a correct description of the environment, and the proper geometric relaxation around the oxygen vacancy, are in an error of less than 0.1 eV for bulk defects. In contrast, standard CASPT2 calculations with rather large basis sets, lead to larger systematic errors (0.5–0.8 eV). The CASPT2 results are affected by the stringent basis set demands of the wave-function-based methods, especially when coupled to the embedding scheme. The further extension of the basis set imposes the use of much larger cluster models, or at least of a larger second shell quantum region, to avoid spurious polarization. In this sense it seems paradoxical that the results that best compare with experiment are those arising from the simplest and less computational demanding method. This seems to be quite a general situation since it has been previously found for the photoinduced desorption of Na and K from SiO_2 (Ref. 26) and very recently in a totally different system such as the gas phase $CuCl_2$ molecule.[70] The accuracy of the prediction for the surface defects is more difficult to establish due to the lack of experimental results.

To summarize, TD-DFT or CASPT2 electronic structure calculations carried out on a properly embedded cluster model having the correct geometric structure of the vacancy relaxation obtained by previous periodic supercell calculations appears to be capable of describing the spectroscopic transitions arising from bulk or surface F and F^+ point defects in α-Al_2O_3.

ACKNOWLEDGMENTS

We thank D. Dominguez-Ariza and J. R. Gomes for stimulating discussions regarding cluster model calculations. This research has been supported by the Spanish DGICYT Grant No. BQU2002-04029-CO2-01 and, in part, by *Generalitat de Catalunya* Grant No. 2001SGR-00043. J.C. thanks the Spanish Ministry of Education for a predoctoral grant. N.L. is grateful to financial support from the MEC through the RyC program. N.L. and F.I. acknowledge support from *Distinció de la Generalitat de Catalunya per a la Promoció de la Recerca Universitària*.

*Author to whom correspondence should be addressed
[1] V. E. Henrich and P. A. Cox, *The Surface Science of Metal Oxides* (Cambridge University Press, Cambridge, 1994).
[2] D. R. Rainer and D. W. Goodman, in *Chemisorption and Reactivity on Suported Clusters and Thin Films: Towards an Understanding of Microscopic Processes in Catalysis*, edited by R. M. Lambert and G. Pacchioni, Vol. 331 of *NATO Advanced Studies Institute, Series E: Applied Sciences* (Kluwer Academic Publishers, Dordrecht, 1997), pp. 27–59.
[3] M. Bäumer, J. Libuda, and H.-J. Freund, in *Chemisorption and Reactivity on Suported Clusters and Thin Films: Towards an Understanding of Microscopic Processes in Catalysis* (Ref. 2), p. 61–104.
[4] H.-J. Freund, Angew. Chem., Int. Ed. **36**, 452 (1997).
[5] C. Barth and M. Reichling, Nature (London) **414**, 54 (2001).
[6] A. Stierle, F. Renner, R. Streitel, H. Dosch, W. Drube, and B. C. Cowie, Science **303**, 1652 (2004).
[7] G. Kresse, M. Schmid, E. Napetschning, M. Shishkin, L. Köhler, and P. Varga, Science **308**, 1440 (2005).
[8] G. Pacchioni, in *The Chemical Physics of Solid Surfaces–Oxide Surfaces*, edited by P. Woodruff (Elsevier, Amsterdam, 2001), Vol. 9, pp. 94–135.
[9] M. Chiesa, M. C. Paganini, E. Giamello, C. Di Valentin, and G. Pacchioni, Angew. Chem., Int. Ed. **42**, 1759 (2003).
[10] R. Schaub, P. Thostrup, N. Lopez, E. Laegsgaard, I. Stensgaard, J. K. Nørskov, and F. Besenbacher, Phys. Rev. Lett. **87**, 266104 (2001).
[11] B. D. Evans and M. Stapelbroek, Phys. Rev. B **18**, 7089 (1978).
[12] K. H. Lee and J. H. Crawford, Phys. Rev. B **15**, 4065 (1977).
[13] K. H. Lee and J. H. Crawford, Appl. Phys. Lett. **33**, 273 (1978).
[14] B. D. Evans, J. Nucl. Mater. **219**, 202 (1995).
[15] A. I. Surdo, V. S. Kortov, and V. A. Pustovarov, Radiat. Meas. **33**, 587 (2001).
[16] S. Y. La, R. H. Bartram, and R. T. Cox, J. Phys. Chem. Solids **34**, 1079 (1973).
[17] A. Stashans, E. Kotomin, and J. L. Calais, Phys. Rev. B **49**, 14 854 (1994).
[18] F. Illas and G. Pacchioni, J. Chem. Phys. **108**, 7835 (1998).
[19] C. Sousa, G. Pacchioni, and F. Illas, Surf. Sci. **429**, 217 (1999).
[20] C. Sousa and F. Illas, J. Chem. Phys. **115**, 1435 (2001).
[21] A. M. Ferrari and G. Pacchioni, J. Phys. Chem. **99**, 17 010 (1995).
[22] E. Scorza, U. Birkenheuer, and C. Pisani, J. Chem. Phys. **107**, 9645 (1997).
[23] P. Mori-Sanchez, J. M. Recio, B. Silvi, C. Sousa, A. Martin Pendas, V. Luaña, and F. Illas, Phys. Rev. B **66**, 075103 (2002).
[24] K. Raghavachari, D. Ricci, and G. Pacchioni, J. Chem. Phys. **116**, 825 (2002).
[25] D. Domínguez-Ariza, C. Sousa, F. Illas, D. Ricci, and G. Pacchioni, Phys. Rev. B **68**, 054101 (2003).
[26] D. Domínguez-Ariza, N. Lopez, F. Illas, G. Pacchioni, and T. E. Madey, Phys. Rev. B **69**, 075405 (2004).
[27] J. Carrasco, J. R. B. Gomes, and F. Illas, Phys. Rev. B **69**, 064116 (2004).
[28] X. G. Wang, A. Chaka, and M. Scheffler, Phys. Rev. Lett. **84**, 3650 (2000).
[29] Z. Łodziana, J. K. Nørskov, and P. Stoltze, J. Chem. Phys. **118**, 11 179 (2003).
[30] Z. Łodziana, N.-Y. Topsøe, and J. K. Nørskov, Nat. Mater. **3**, 289 (2004).
[31] J. P. Perdew and Y. Wang, Phys. Rev. B **45**, 13 244 (1992).
[32] P. E. Blöchl, Phys. Rev. B **50**, 17 953 (1994).
[33] G. Kresse and D. Joubert, Phys. Rev. B **59**, 1758 (1999).
[34] J. Carrasco, N. Lopez, and F. Illas, Phys. Rev. Lett. **93**, 225502 (2004).
[35] G. Kresse and J. Furthmüller, Comput. Mater. Sci. **6**, 15 (1996).
[36] G. Kresse and J. Hafner, Phys. Rev. B **47**, R558 (1993); G. Kresse and J. Furthmüller, *ibid.* **54**, 11 169 (1996).
[37] C. Sousa, J. Casanovas, J. Rubio, and F. Illas, J. Comput. Chem. **14**, 680 (1993).
[38] G. Pacchioni, A. M. Ferrari, A. M. Marquez, and F. Illas, J. Comput. Chem. **18**, 617 (1996).
[39] C. de Graaf, C. Sousa, and F. Illas, *Computational Materials Science*, edited by C. R. A. Catlow and E. Kotomin, Vol. 187 of *NATO Series III: Computers and System Sciences* (IOS Press, Amsterdam 2003), p. 167–195.
[40] C. Sousa, C. de Graaf, N. Lopez, N. M. Harrison, and F. Illas, J. Phys.: Condens. Matter **16**, S2557 (2004).
[41] F. Illas, I. de P. R. Moreira, C. de Graaf, O. Castell, and J. Casanovas, Phys. Rev. B **56**, 5069 (1997).
[42] I. de P. R. Moreira, F. Illas, C. J. Calzado, J. F. Sanz, J. P. Malrieu, N. Ben Amor, and D. Maynau, Phys. Rev. B **59**, R6593 (1999).
[43] P. Ewald, Ann. Phys. **64**, 253 (1921).
[44] J. R. B. Gomes, F. Illas, N. Cruz Hernández, A. Marquez, and J. F. Sanz, Phys. Rev. B **65**, 125414 (2002).
[45] A. D. Becke, J. Chem. Phys. **98**, 5648 (1993); C. Lee, W. Yang, and R. G. Parr, Phys. Rev. B **37**, 785 (1993).
[46] J. Q. Broughton and P. S. Bagus, Phys. Rev. B **36**, 2813 (1987).
[47] W. R. Wadt and P. J. Hay, J. Chem. Phys. **82**, 284 (1985).
[48] A. Schafer, H. Horn, and R. Ahlrichs, J. Chem. Phys. **97**, 2571 (1992).
[49] See http://www.emsl.pnl.gov/forms/basisform.html
[50] M. J. Frisch *et al.*, *Gaussian98.A7* (Gaussian, Pittsburgh, PA, 1998).
[51] K. Andersson, P. A. Malmqvist, B. O. Roos, A. J. Sadlej, and K. Wolinski, J. Phys. Chem. **94**, 5483 (1990).
[52] K. Andersson, P. A. Malmqvist, and B. O. Roos, J. Phys. Chem. **96**, 1218 (1992).
[53] C. de Graaf, R. Broer, and W. C. Nieuwpoort, Chem. Phys. **208**, 35 (1996).
[54] C. de Graàf and R. Broer, Phys. Rev. B **62**, 702 (2000).
[55] C. Sousa, C. de Graaf, and F. Illas, Phys. Rev. B **62**, 10 013 (2000).
[56] C. Sousa, C. de Graaf, and G. Pacchioni, J. Chem. Phys. **114**, 6259 (2001).
[57] C. de Graaf, C. Sousa, I. de P. R. Moreira, and F. Illas, J. Phys. Chem. A **105**, 11 371 (2001).
[58] C. Sousa, C. de Graaf, F. Illas, M. T. Barriuso, J. A. Aramburu, and M. Moreno, Phys. Rev. B **62**, 13 366 (2000).
[59] J. L. Pascual, L. Seijo, and Z. Barandiaran, J. Chem. Phys. **100**, 2010 (1994).
[60] K. Andersson, M. Barysz, A. Bernhardsson, M. R. A. Blomberg, D. L. Cooper, T. Fleig, M. P. Fülscher, C. de Graaf, B. A. Hess, G. Karlström, R. Lindh, P.-Å. Malmqvist, P. Neográdi, J. Olsen, B. O. Roos, B. Schimmelpfennig, M. Schütz, L. Seijo, L. Serrano-Andrés, P. E. M. Siegbahn, J. Starling, T. Thorsteinsson, V. Veryazov, and P.-O. Widmark, MOLCAS version 5.2, University of Lund, Sweden, 2000.
[61] C. Sousa, F. Illas, and G. Pacchioni, J. Chem. Phys. **99**, 6818 (1993).

[62] R. Baxter, P. Reinhardt, N. Lopez, and F. Illas, Surf. Sci. **445**, 448 (2000).
[63] J. R. B. Gomes, I. de P. R. Moreira, P. Reinhardt, A. Wander, B. G. Searle, N. M. Harrison, and F. Illas, Chem. Phys. Lett. **341**, 412 (2001).
[64] I. P. R. Moreira, F. Illas, and R. L. Martin, Phys. Rev. B **65**, 155102 (2002).
[65] R. H. French, J. Am. Ceram. Soc. **73**, 477 (1990).
[66] A. Larsson, Ph.D. thesis, Chalmers University, Göteborg, Sweden, 2000.
[67] J. Muscat, A. Wander, and N. M. Harrison, Chem. Phys. Lett. **342**, 397 (2001).
[68] D. Peterka, C. Tegenkamp, K. M. Schroder, W. Ernst, and F. Pfnur, Surf. Sci. **431**, 146 (1999).
[69] W. P. Hess, A. G. Joly, K. M. Beck, P. V. Sushko, and A. L. Shluger, Surf. Sci. **564**, 62 (2004).
[70] A. Ramirez-Solis, R. Poteau, A. Vela, and J. P. Daudey, J. Chem. Phys. **122**, 164306 (2005).